Frontiers of Information Technology & Electronic Engineering
www.jzus.zju.edu.cn; engineering.cae.cn; www.springerlink.com
ISSN 2095-9184 (print); ISSN 2095-9230 (online)
E-mail: jzus@zju.edu.cn

Correspondence:

A novel wideband ring antenna for polarization/pattern diversity*

Li SUN†‡[1], Shigang ZHOU[1], Guanxi ZHANG[2], Baohua SUN[3]

[1]*School of Microelectronics, Northwestern Polytechnical University, Xi'an 710072, China*

[2]*Huawei Technologies Co., Ltd., Shanghai 201206, China*

[3]*National Key Laboratory of Antennas and Microwave Technology, Xidian University, Xi'an 710071, China*

†E-mail: lisun@nwpu.edu.cn

Received Sept. 3, 2021; Revision accepted Dec. 7, 2021; Crosschecked Jan. 28, 2022

https://doi.org/10.1631/FITEE.2100421

We present a novel wideband ring antenna for polarization/pattern diversity. The proposed antenna consists of eight printed dipole elements in the form of a circular array. The arms of adjacent elements overlap for capacitive loading. Unlike traditional circular arrays, a method of exciting elements in the form of every two intervals is first introduced. We prove that this method can maintain the wideband characteristics of the antenna. Four independent feeding ports in a ring antenna aperture are designed for the polarization/pattern diversity with suitable feeding networks. As an example, a wideband dual-polarized antenna was designed based on the proposed ring antenna. To achieve two orthogonal linear polarizations with maximum radiation in the Z direction, two adjacent elements are extracted periodically to feed through one port. The differential feeding network and integrated Baluns have been designed to realize broadside radiation patterns, considering impedance and phase matching. Because the proposed antenna is hollow, it is a good candidate for a multiband sharing aperture antenna element. Results show that the proposed antenna has an overlapped bandwidth of 50.5% (1.04–1.82 GHz) with voltage standing wave ratio (VSWR)< 2 for the two polarizations, and port isolation less than 23 dB. The measured realized gain ranges from 6.1 to 8.1 dBi, with stable broadside radiation patterns over the operating frequency band.

1 Introduction

Wideband antennas are attracting a lot of attention in both communication and radar systems with their advantages of high channel capacity, superior resolution, and precise ranging. Meanwhile, polarization/pattern diversity can increase communication capability. Therefore, many attempts have been made to develop antennas that have wideband and polarization/pattern diversity.

Conventional wideband dual-polarized antennas such as sinuous antennas (Zheng et al., 2018), log-periodic antennas (Liang et al., 2014), and Vivaldi antennas (Dong et al., 2018; Tianang et al., 2020) obtained wideband characteristics by using elements with inherent broad bandwidth. In Dong et al. (2018), a Vivaldi antenna with pattern diversity across the entire band from 0.7 to 2.7 GHz has been described. However, its considerable height limits its applications. Magneto-electric dipoles (Wu and Luk, 2016; Gao et al., 2019) with low-profile characteristics are a

‡ Corresponding author

* Project supported by the National Natural Science Foundation of China (Nos. 61901255 and 61771395), the Taicang City Natural Science Foundation of China (No. TC2020JC09), the Shaanxi Provincial Natural Science Foundation of China (No. 2018JM6085), and the Starting Research Fund from the Northwestern Polytechnical University, China (No. D5000210622)

ORCID: Li SUN, https://orcid.org/0000-0002-5259-9532

type of wideband dual-polarized antenna. In Gao et al. (2019), a polarized reconfigurable magneto-electric dipole antenna was achieved by introducing PIN diodes. Nevertheless, they are not helpful for pattern diversity, since they usually obtain unidirectional radiation patterns based on the operation theory. Another type of wideband dual-polarized antenna is tightly coupled dipole arrays (TCDAs). TCDAs are usually one-dimensional (1D) (Lee and Nam, 2017; Kim and Nam, 2019) or two-dimensional (2D) (Zhong et al., 2019) structures, achieving wideband and dual-polarized characteristics by strong coupling between the elements. However, for good performance, the number of elements must be sufficient, and the current truncation effects of edge elements must be considered.

With the advantage of exciting different working modes, wideband patch antennas (Huang H et al., 2014; Huang HJ et al., 2020; Liu et al., 2021) have been widely investigated for pattern diversity. To obtain dual-polarization characteristics, multi-port antennas have been designed (Al-Rawi et al., 2014; Satam and Nema, 2017; Parchin et al., 2020). For spatial/polarization diversity, a circularly polarized multiple-input multiple-output (MIMO) ultra-wideband antenna has been proposed (Ullah et al., 2020). By simply switching the position of the ground plane of the feed line, both the radiation patterns and polarization can be changed.

In this study, we present a wideband ring antenna. Unlike in traditional circular arrays, a method of exciting elements at every two intervals is first introduced. Results show that discontinuous units according to the state of every two intervals to feed at the same time could obtain the wideband characteristic. Therefore, a wideband ring antenna for dual-polarization has been designed using exciting and terminal loaded elements. The proposed antenna consists of eight printed dipole elements in the form of a circular array. To achieve dual-polarization characteristics, discontinuous units are extracted periodically to feed through one port in the proposed antenna. As a result, the eight elements are divided into two orthogonal groups with the same structure, realizing two orthogonal linear polarizations. When one polarization is excited, the other non-fed elements are terminal loaded, mitigating the current truncation effects to obtain wideband characteristics. Different radiation patterns can be obtained by changing the exciting phase of the elements. For example, for securing broadside radiation patterns for each polarization, the non-adjacent elements should be excited with out-of-phase signals, which are obtained by designing a proper differential feeding network and integrated Baluns. Results show that both wideband and dual-polarized characteristics can be achieved with the proposed antenna.

2 Theoretical analysis of the proposed ring antenna

Overlapping dipole elements are used to increase the bandwidth of a ring antenna. First, a finite 1×4 linear dipole array with overlapping arms is analyzed (Fig. 1). The dipole element is excited by a lumped port between the two arms. A metal ground plane is placed under the dipole. The height of the dipole controls its self-inductance, and the coupling capacitance is created by the overlap of the dipole arms, which are printed on the opposite sides of the supporting substrate, with a thickness of 0.254 mm and a relative dielectric constant of 2.2. The total height of the substrate is 80 mm. The width of the dipole (W) is 17 mm and the length (L) is 24 mm. The parameters are selected based on simulation analysis, in which the commercial simulation software ANSYS HFSS is used, considering antenna size and bandwidth characteristics.

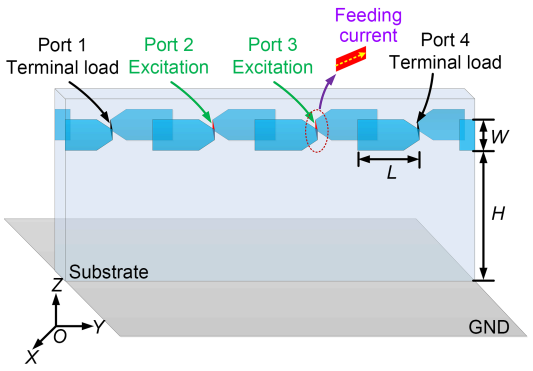

Fig. 1 Schematic of the dipole array with arms overlapped

As the symmetry of the model, the simulated VSWR of port P2 is illustrated in Fig. 2 with different working states of the edge elements. A parameter

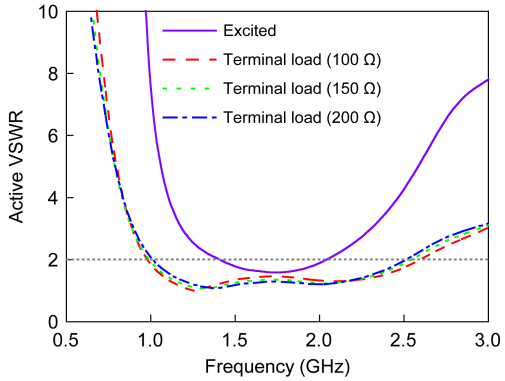

Fig. 2 Simulated active VSWR for port P2 of the dipole array with arms overlapped

analysis of the terminal load is shown in Fig. 2. Since the port impedance of the excitations is chosen as 150 Ω, a similar terminal load impedance is selected. When the edge elements are excited, a low active VSWR of port P2 is obtained, with a bandwidth of 35.5%. The bandwidth of the finite antenna array is worse because mutual coupling diminishes near the edges of the array. Terminating the edge elements with matched resistors is an effective method to address this issue. When the edge elements are terminated in 150 Ω resistors, a bandwidth of about 88.9% is obtained. Changing the values of the terminal load resistors from 100 to 200 Ω has a weak effect on the active VSWR (Fig. 2).

The terminal loaded technique can obtain better active impedance matching of the middle elements. However, the edge elements are not used effectively since they are not excited. For total usage of the terminal loaded elements, a ring antenna consisting of eight dipole elements is proposed. A schematic of the proposed antenna is illustrated in Fig. 3. Eight dipoles

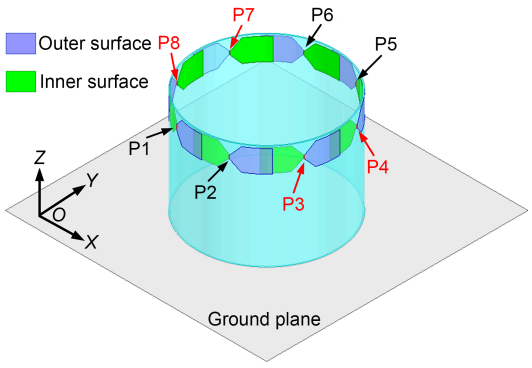

Fig. 3 Schematic of the proposed ring antenna

are tightly and uniformly arranged on a circular substrate. The sizes of the dipole elements and the cylindrical substrate used are similar to those of a 1×4 linear dipole array. The excited lumped ports are connected to the two arms of each element, with the port name marked in Fig. 3. The eight ports are divided into two groups: ports P1, P2, P5, and P6 in one group, and the remaining ports in the other group. One group of ports is excited to obtain wideband characteristics while the other is terminal loaded, and vice versa. Each group of antenna elements has the same current direction, forming one linear polarization. Therefore, a dual-polarized wideband is obtained based on the proposed ring antenna. The dual-polarization characteristic is achieved by exchanging the working states of the two groups of elements. In addition, different radiation patterns can be obtained by changing the magnitude and phase of the ports. To prove this, three cases with different phases are analyzed. When one group's ports are excited, two adjacent elements maintain an excitation of equal amplitude, while the other adjacent elements change the exciting phase from 0° to 90° to 180°. Table 1 shows the exciting amplitude and phase of ports under different cases. Though all ports display excitation information, only one group of ports is excited each time. Fig. 4 shows the simulation results of the radiation patterns for the two groups of ports for three cases. The radiation patterns change with the different exciting phases of the radiated elements. Fig. 5 shows the active VSWR of each case. The active VSWR is influenced by the exciting phase, but it could maintain the wideband characteristic.

Table 1 Different cases of the feeding ports (amplitude/phase)

Case	P1	P2	P3	P4	P5	P6	P7	P8
1	1/0°	1/0°	1/0°	1/0°	1/0°	1/0°	1/0°	1/0°
2	1/0°	1/0°	1/0°	1/0°	1/90°	1/90°	1/90°	1/90°
3	1/0°	1/0°	1/0°	1/0°	1/180°	1/180°	1/180°	1/180°

3 Application of the wideband dual-polarized antenna with broadside radiation pattern

The proposed ring antenna has been designed for polarization diversity with broadside radiation

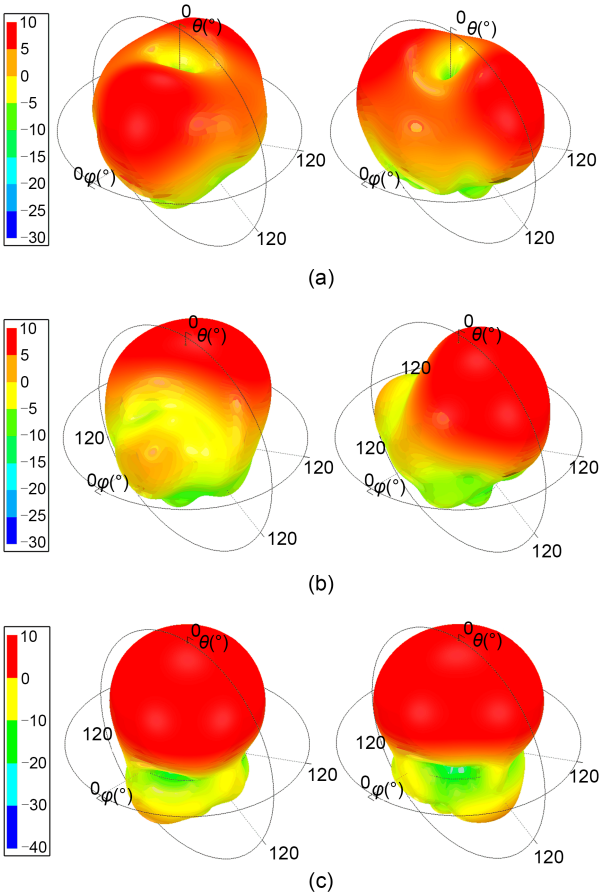

Fig. 4 Simulated 3D radiation patterns of the gain for three cases: (a) case 1; (b) case 2; (c) case 3

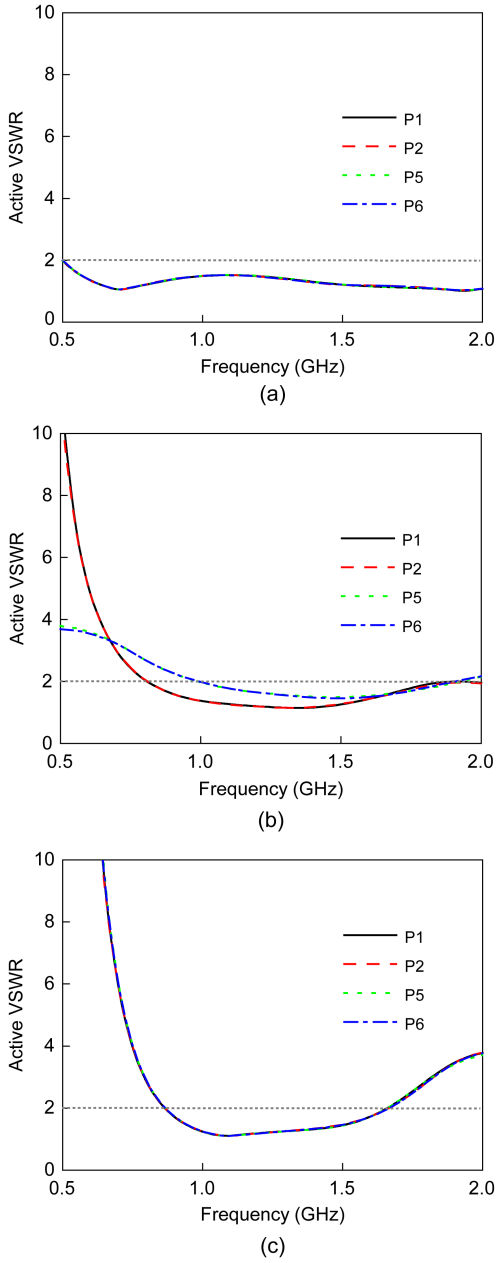

Fig. 5 Simulated active VSWR for three cases: (a) case 1; (b) case 2; (c) case 3

patterns along the Z axis. To obtain two orthogonal polarization, the eight elements are divided into two groups periodically based on pairs of adjacent elements. As a result, ports P1, P2, P5, and P6 are extracted as one group marked in black, and ports P3, P4, P7, and P8 are extracted as the other group, marked in red. When the four ports in one group are excited, the four in the other group are terminal loaded. Since the exciting impedance is 150 Ω, the value of the terminal load is chosen as 150 Ω as well. To obtain current in the same direction, the symmetric lumped ports in one group should be excited with out-of-phase signals, as marked in Fig. 6. Using this special discontinuous feeding mode, the array maintains the wideband characteristic. Moreover, the dual-polarization feature is achieved by exchanging the working states of the two groups of elements. The simulated active VSWR results for excited ports P1, P2, P5, and P6 are shown in Fig. 7a. Ports P1 and P2 are excited with the 0° phase, while ports P5 and P6 are excited with the 180° phase. Ports P3, P4, P7, and P8 are loaded with 150 Ω resistors. All the excited ports show similar results: the operating band of the exciting ports for active VSWR<2 is from 0.93 to 1.94 GHz. Therefore, linear polarization along the X axis is obtained. On the other hand, to obtain orthogonal linear polarization along the Y axis, the exciting ports and terminal loaded ports need to be exchanged. That is

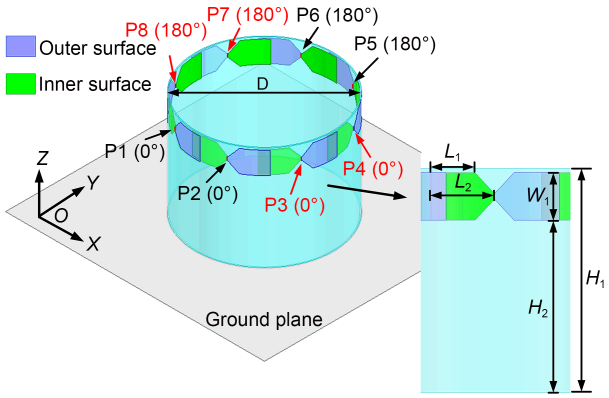

Fig. 6 Schematic of the dual-polarized ring antenna

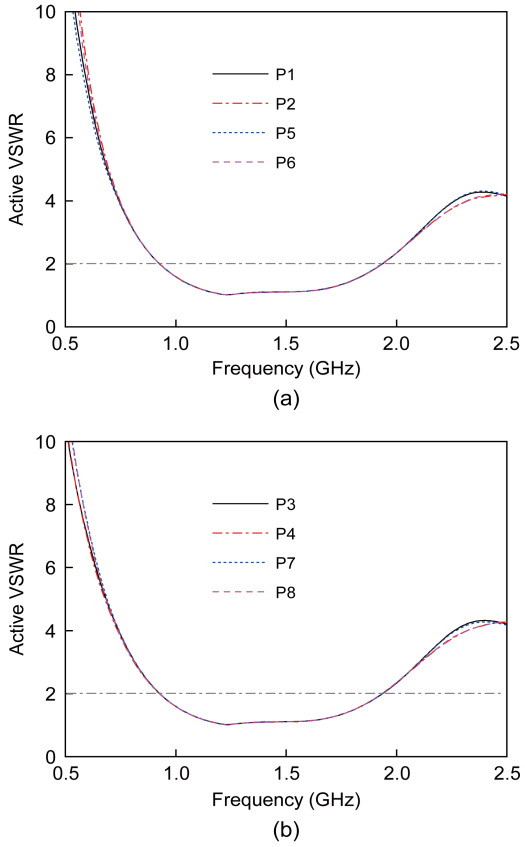

Fig. 7 Simulated active VSWR of the dual-polarized ring antenna for polarization along the *X* axis (a) and *Y* axis (b)

to say, ports P3 and P4 are excited with the 0° phase while ports P7 and P8 are excited with the 180° phase. The non-excited ports are terminated with 150 Ω resistors. The simulated active VSWR results for polarization along the *Y* axis are shown in Fig. 7b. Due to the symmetry of the circular array structure, the same simulation results are obtained.

To verify the surface current distribution, the simulated current distribution at 1.5 GHz for polarization along the *X* and *Y* axes is shown in Fig. 8. When ports P1, P2, P5, and P6 are excited with the same amplitude and opposite phase, the sum vector of the current surface points along the *X* axis. When ports P3, P4, P7, and P8 are excited with the same amplitude and opposite phase, the sum vector of the current surface points along the *Y* axis. As the sum vectors of the surface current in the two states are orthogonal, the isolation of the two polarizations is sound. Therefore, a wideband dual-polarized ring antenna with a broadside radiation pattern can be achieved by feeding the discontinuous units according to adjacent every two.

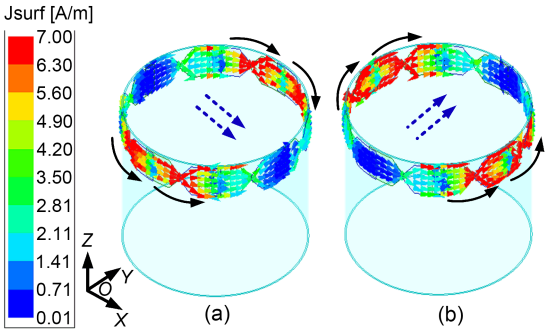

Fig. 8 Simulated current distribution at 1.5 GHz of the dual-polarized ring antenna for polarization along the *X* axis (a) and *Y* axis (b)

Based on the analysis above, the proposed dual-polarized antenna was designed. The computational model of the antenna was implemented and simulated using ANSYS HFSS. The detailed configuration of the proposed antenna is shown in Fig. 9, with the dimensions listed in Table 2. Eight dipoles and tapered

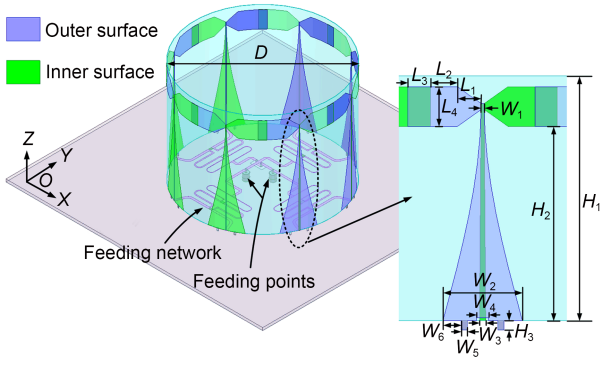

Fig. 9 Schematic of the dual-polarized antenna

Table 2 Detailed parameters of the proposed antenna

Parameter	Value (mm)	Parameter	Value (mm)
W_1	0.4	L_2	11.4
W_2	22.4	L_3	4.8
W_3	0.6	L_4	13.0
W_4	3.0	H_1	80.0
W_5	2.0	H_2	63.5
W_6	5.0	H_3	3.0
L_1	6.8	D	106.0

Baluns were printed on a circular substrate with a diameter of D. The substrate was chosen as RT5880 with a dielectric constant of 2.2 and thickness of 0.254 mm. The balanced ports of the Baluns were connected to the dipole elements, while their unbalanced ports were connected to the corresponding output of the feeding network. The Baluns need to be properly designed because they are acting as combining signals and transforming impedance. Both the microstrip and the ground of the Balun were chosen as index gradient-type. By tuning the width of the microstrip, the Balun can transform the balanced 150 Ω input impedance of the antenna to 100 Ω, matching the unbalanced output impedance of the feeding network. As shown in Fig. 9, the grounds of four adjacent Baluns were printed on the outer surface of the circular substrate, while the grounds of the other four Baluns were printed on the inner surface of the substrate. By this design, the symmetrical dipole elements had the differential phase without adding extra 180° phase shifters through the feeding network. To connect the ground of the Balun to the ground of the feeding network, which was printed on the underside of the substrate, metalized rectangular bars were added on each ground of the Balun. The metalized rectangular bars also served to fix the circular substrate. To prevent the tapered microstrip from being shorted, a rectangular slot was hollowed out on each ground of the Balun.

The feeding network was based on the Wilkinson power divider design. A schematic of the proposed feeding network is shown in Fig. 10, with the detailed parameters listed in Table 3. It was printed on a square substrate with a side length of 250 mm. The chosen substrate was F4BM-2 with a dielectric constant of 2.65 and thickness of 2 mm. The feeding network was printed on the top side of the substrate, while its ground was printed on the underside,

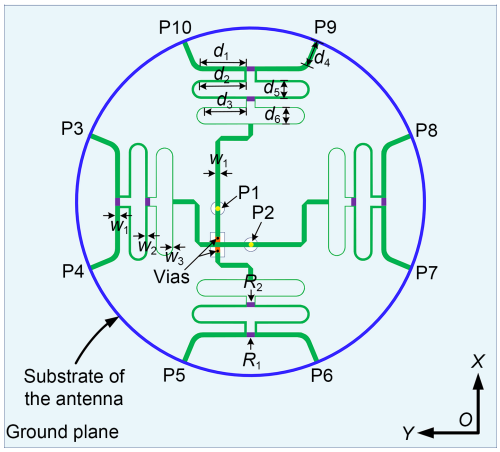

Fig. 10 Schematic of the feeding network

Table 3 Detailed parameters of the feeding network

Parameter	Value	Parameter	Value	Parameter	Value
w_1 (mm)	1.5	d_2 (mm)	17.5	d_6 (mm)	4.6
w_2 (mm)	1	d_3 (mm)	13.7	R_1 (Ω)	300
w_3 (mm)	0.385	d_4 (mm)	9	R_2 (Ω)	200
d_1 (mm)	14.7	d_5 (mm)	4		

connecting to the Balun grounds through metalized rectangular bars. The two input ports (P1 and P2) were directly fed by the 50 Ω SubMiniature version A (SMA) connectors, and the output ports (P3–P10) were welded to the unbalanced ports of the Baluns. The simulated S parameter results of the feeding network are shown in Fig. 11. As shown in Fig. 11a, two input ports each had return losses of less than 15 dB and isolations of more than 20 dB from 0.82 to 1.93 GHz. Furthermore, the input power was divided into four output ports equally with the power division of 6±0.25 dB from 0.82 to 1.93 GHz, satisfying the bandwidth requirements of the proposed dual-polarized antenna. Finally, the proposed dual-polarized antenna was achieved with full consideration of the Baluns and the feeding network.

Based on the designed structure, the proposed dual-polarized antenna was fabricated and measured. A picture of the fabricated antenna is shown in Fig. 12, with its simulated and measured S parameter results shown in Fig. 13. The 10-dB bandwidth was from 1.04 to 1.82 GHz for each port, with isolation less than 23 dB, which agrees reasonably well with the simulation results. At 1.2, 1.4, and 1.6 GHz, the simulated and measured radiation patterns for P1 in the

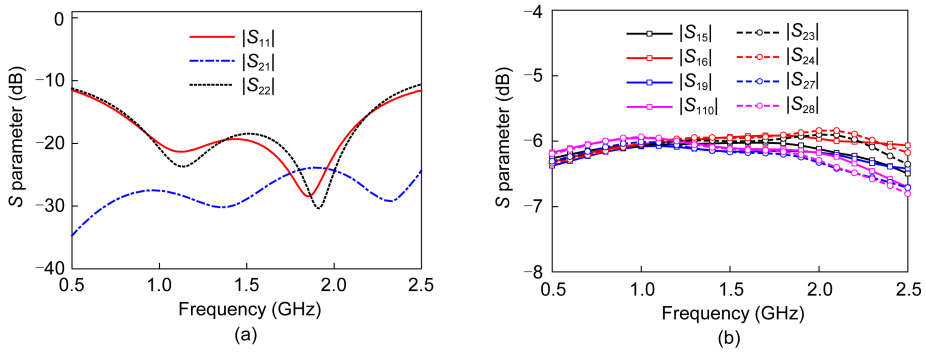

Fig. 11 Simulated *S* parameter of the feeding network: (a) input ports; (b) output ports

Fig. 12 A picture of the fabricated antenna along the *Y* axis

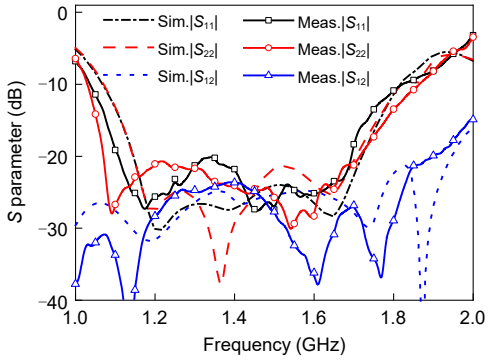

Fig. 13 Simulated and measured *S* parameters of the proposed antenna

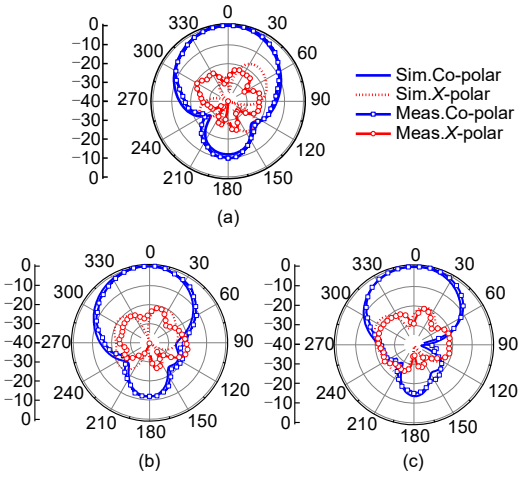

Fig. 14 Simulated and measured radiation patterns of the proposed antenna in the *XOZ* plane with port P1 excited at 1.2 GHz (a), 1.4 GHz (b), and 1.6 GHz (c)

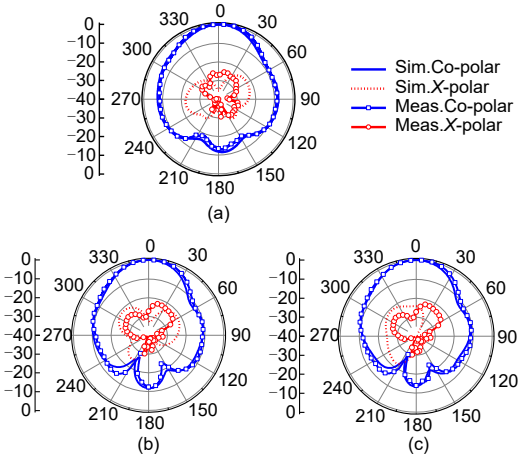

Fig. 15 Simulated and measured radiation patterns of the proposed antenna in the *YOZ* plane with port P1 excited at 1.2 GHz (a), 1.4 GHz (b), and 1.6 GHz (c)

XOZ and *YOZ* planes are illustrated in Figs. 14 and 15, respectively. Those for P2 are illustrated in Figs. 16 and 17. When one port was measured, the other port was connected to a 50 Ω resistor, acting as terminal load on the non-excited elements. The measured radiation patterns showed reasonably good agreement along the co- and cross-polarization, and the broadside and stable radiation patterns achieved cover the whole operating band. The measured cross-polarization levels within the main lobe were less than −20 dB for both the E-plane and H-plane, while the front-to-back ratio remained over 12 dB. The simulated and measured gains of the antenna are shown in Fig. 18. The measured gain was slightly lower than the simulated value, ranging from 6.1 to 8.1 dBi, with a gain variation of about 2 dB over the operating band. The simulated

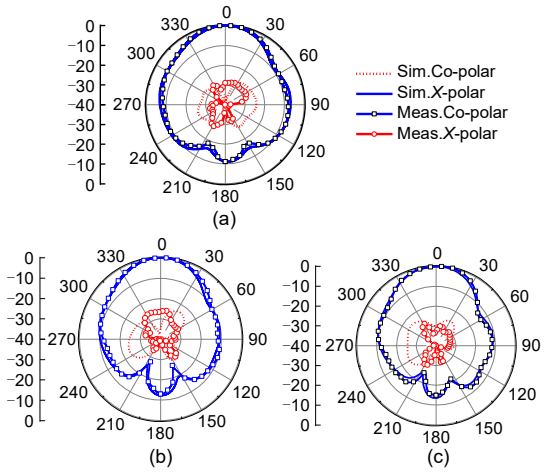

Fig. 16 Simulated and measured radiation patterns of the proposed antenna in the *XOZ* plane with port P2 excited at 1.2 GHz (a), 1.4 GHz (b), and 1.6 GHz (c)

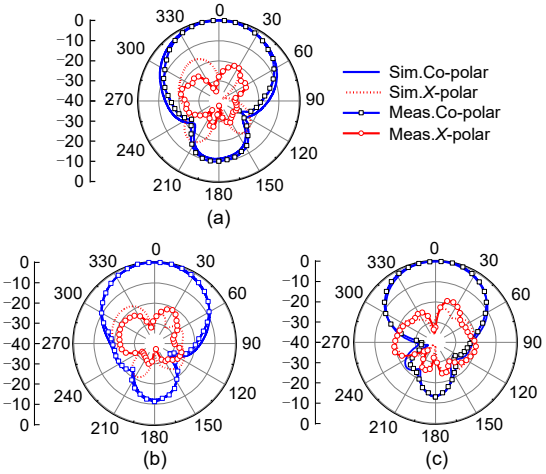

Fig. 17 Simulated and measured radiation patterns of the proposed antenna in the *YOZ* plane with port P2 excited at 1.2 GHz (a), 1.4 GHz (b), and 1.6 GHz (c)

and measured efficiencies of the antenna are shown in Fig. 19. The total efficiency is a combination of the radiation and mismatch efficiencies. The efficiency in the middle of the working frequency was lower than that at the other working frequency, which was caused by the absorption resistances of the feeding network. Therefore, the measured efficiency was lower than that of the simulation. The discrepancy between the simulated and measured efficiency is likely due to manufacturing and measurement errors. Nevertheless, the measured efficiency remained over 75% in the whole working band.

To illustrate the advantages of the dual-polarized antenna proposed in this study, Table 4 presents a

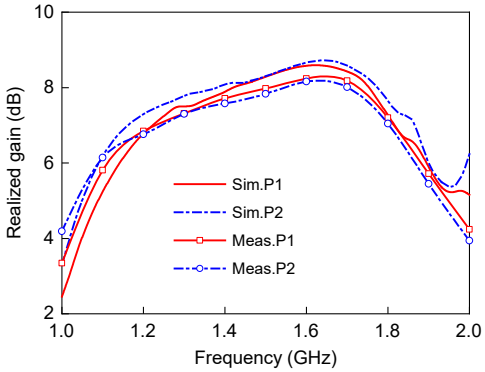

Fig. 18 Simulated and measured gains of the proposed dual-polarized antenna

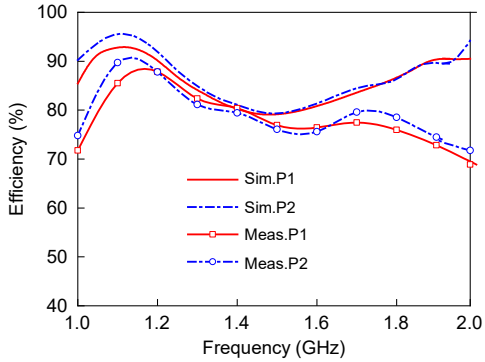

Fig. 19 Simulated and measured efficiencies of the proposed dual-polarized antenna

comparison of the performance of this antenna with those of previous reports. The proposed antenna has a wideband, small size, and good impedance matching and radiation characteristics. Furthermore, with more units in one aperture, it is easier to tune the operating characteristics (polarization/pattern diversity) according to requirements.

4 Conclusions

A novel wideband ring antenna for polarization/pattern diversity has been introduced in this paper. By arranging overlapping dipole elements in a circular array, multiple ports exist in one aperture. Unlike in traditional circular arrays, a method of exciting elements in the form of every two intervals was first introduced, in which the broadband characteristics of the antenna are realized. We proved theoretically that this method can maintain the wideband characteristics of the antenna. As a result, the proposed antenna

Table 4 Performance comparisons between this work and previous reports

Reference	Antenna type	Bandwidth	Realized gain (dBi)	Size (λ_{lowest})	Isolation	Cross-polarization	Number of units
Zheng et al. (2018)	Sinuous antenna	85.7%	6–8.2	$0.33\lambda^2\times\lambda$	–	>15 dB	4
Liang et al. (2014)	Log periodic antenna	Cover 2.4/5 WLAN	5/6	$1.28\lambda^2\times0.48\lambda$	>30 dB	>15 dB	12
Tianang et al. (2020)	Vivaldi antenna	120%	8–16	$0.36\lambda^2\times0.8\lambda$	>35 dB	>30 dB	3
Wu and Luk (2016)	Magneto-electric dipole	48%	7.7–11	$0.52\lambda^2\times0.15\lambda$	>30 dB	>22 dB	2
Kim and Nam (2019)	1D tightly coupled array	103%	7.7–12.4	$1.69\lambda\times0.59\lambda\times0.13\lambda$	–	–	22
Ullah et al. (2020)	MIMO monopoles	82%	2–6	$0.34\lambda^2$	>20 dB	–	2
This work	Wideband ring antenna	55.5%	6.1–8.1	$0.37\lambda^2\times0.28\lambda$	>23 dB	>20 dB	4

can be designed for polarization/pattern diversity with proper feeding networks. As an example, a wideband dual-polarized antenna with a broadside radiation pattern was designed and analyzed. The dual-polarized characteristics were obtained by exciting different elements in the circular array. The good results obtained showed that the proposed antenna can be used in wireless communication application scenarios such as conference rooms and stadiums.

Contributors

Li SUN designed the research. Guanxi ZHANG guided the research. Li SUN processed the data. Li SUN and Shigang ZHOU drafted the paper. Shigang ZHOU, Guanxi ZHANG, and Baohua SUN revised the paper. Shigang ZHOU finalized the paper.

Compliance with ethics guidelines

Li SUN, Shigang ZHOU, Guanxi ZHANG, and Baohua SUN declare that they have no conflict of interest.

References

Al-Rawi A, Hussain A, Yang J, et al., 2014. A new compact wideband MIMO antenna—the double-sided tapered self-grounded monopole array. *IEEE Trans Antenn Propag*, 62(6):3365-3369. https://doi.org/10.1109/TAP.2014.2309985

Dong YD, Choi J, Itoh T, 2018. Vivaldi antenna with pattern diversity for 0.7 to 2.7 GHz cellular band applications. *IEEE Antenn Wirel Propag Lett*, 17(2):247-250. https://doi.org/10.1109/LAWP.2017.2783323

Gao S, Lin HW, Ge L, et al., 2019. A magneto-electric dipole antenna with switchable circular polarization. *IEEE Access*, 7:40013-40018. https://doi.org/10.1109/ACCESS.2019.2905629

Huang H, Liu Y, Zhang SS, et al., 2014. Uniplanar differentially driven ultrawideband polarization diversity antenna with band-notched characteristics. *IEEE Antenn Wirel Propag Lett*, 14:563-566. https://doi.org/10.1109/LAWP.2014.2374332

Huang HJ, Gao S, Lin SH, et al., 2020. A wideband water patch antenna with polarization diversity. *IEEE Antenn Wirel Propag Lett*, 19(7):1113-1117. https://doi.org/10.1109/LAWP.2020.2990226

Kim S, Nam S, 2019. Bandwidth extension of dual-polarized 1-D TCDA antenna using VMS. *IEEE Trans Antenn Propag*, 67(8):5305-5312. https://doi.org/10.1109/TAP.2019.2916745

Lee H, Nam S, 2017. A dual-polarized 1-D tightly coupled dipole array antenna. *IEEE Trans Antenn Propag*, 65(9): 4511-4518. https://doi.org/10.1109/TAP.2017.2723262

Liang JJ, Hong JS, Zhao JB, et al., 2014. Dual-band dual-polarized compact log-periodic dipole array for MIMO WLAN applications. *IEEE Antenn Wirel Propag Lett*, 14: 751-754. https://doi.org/10.1109/LAWP.2014.2378772

Liu JF, Weng ZB, Zhang ZQ, et al., 2021. A wideband pattern diversity antenna with a low profile based on metasurface. *IEEE Antenn Wirel Propag Lett*, 20(3):303-307. https://doi.org/10.1109/LAWP.2020.3048633

Parchin NO, Basherlou HJ, Al-Yasir YIA, et al., 2020. Ultra-wideband MIMO diversity antenna system for future handsets. Proc 14th European Conf on Antennas and Propagation, p.1-4. https://doi.org/10.23919/EuCAP48036.2020.9135613

Satam V, Nema S, 2017. Dual polarized four element diversity antenna for UWB applications. Proc IEEE Int Conf on Antenna Innovations & Modern Technologies for Ground, Aircraft and Satellite Applications, p.1-5. https://doi.org/10.1109/IAIM.2017.8402527

Tianang EG, Elmansouri MA, Filipovic DS, 2020. Ultrawideband flush-mountable dual-polarized Vivaldi antenna. *IEEE Trans Antenn Propag*, 68(7):5670-5674. https://doi.org/10.1109/TAP.2019.2963216

Ullah U, Mabrouk IB, Koziel S, et al., 2020. Implementation of spatial/polarization diversity for improved-performance circularly polarized multiple-input-multiple-output ultra-wideband antenna. *IEEE Access*, 8:64112-64119. https://doi.org/10.1109/ACCESS.2020.2984697

Wu F, Luk KM, 2016. A reconfigurable magneto-electric dipole antenna using bent cross-dipole feed for polarization diversity. *IEEE Antenn Wirel Propag Lett*, 16:412- 415. https://doi.org/10.1109/LAWP.2016.2581259

Zheng SF, Gao S, Yin YZ, et al., 2018. A broadband dual circularly polarized conical four-arm sinuous antenna. *IEEE Trans Antenn Propag*, 66(1):71-80. https://doi.org/10.1109/TAP.2017.2772301

Zhong JN, Johnson A, Alwan EA, et al., 2019. Dual-linear polarized phased array with 9:1 bandwidth and 60° scanning off broadside. *IEEE Trans Antenn Propag*, 67(3): 1996-2001. https://doi.org/10.1109/TAP.2019.2891607